Formation of metal nanoparticles in silicon nanopores: Plasmon resonance studies

S. Polisski,[1,a)] B. Goller,[1] S. C. Heck,[2] S. A. Maier,[2] M. Fujii,[3] and D. Kovalev[1]
[1]*Department of Physics, University of Bath, Bath BA2 7AY, United Kingdom*
[2]*Department of Physics, Imperial College London, London SW7 2AZ, United Kingdom*
[3]*Department of Electrical and Electronics Engineering, Kobe University, Rokkodai, Nada, Kobe 657-8501, Japan*

(Received 24 November 2010; accepted 20 December 2010; published online 6 January 2011)

We present a method for the formation of noble metal nanoparticle ensembles in nanostructured silicon. The key idea is based on the unique property of the large reduction potential of extended internal hydrogen-terminated porous silicon surfaces. The process of metal nanoparticle formation in porous silicon was experimentally traced using their optical plasmon resonance response. We also demonstrate that bimetallic compounds can be formed in porous silicon and that their composition can be controlled using this technique. Experimental results were found to contradict partially with considerations based on Mie theory. © *2011 American Institute of Physics*. [doi:10.1063/1.3537811]

Noble metal nanostructures have very specific optical properties due to localized surface plasmon resonances (LSPRs), light-induced collective oscillations of their conduction electrons.[1] The optical properties of gold (Au) and silver (Ag) nanoparticles (NPs) have been extensively studied, as their LSPR lies in the visible spectrum as long as the particles are ~100 nm or less.[1] Plasmonics is a growing field with applications in biology using the effect of surface enhanced Raman scattering (SERS),[2] photovoltaics,[3] and catalysis,[4,5] among others. Metal NPs can be deposited on various supporting substrates or chemically synthesized by the reduction in metal salt.[6] In contrast to common chemical methods, which require the presence of reducing agents and stabilizers, in porous silicon (PSi) metal NPs are formed without their addition.

In this paper we demonstrate that NPs of Au, platinum (Pt), and a mixture of both can be synthesized in PSi in a controllable way. This technique employs the large reduction potential of extended hydrogen-terminated surface of PSi to reduce the metal salt, resulting in the formation of metal NPs inside the pores. NP growth can be controlled by the PSi matrix (selection of pore size distribution), metal salt concentration, and exposure time.

Freestanding PSi layers have been prepared in HF-ethanol solutions via standard electrochemical etching[7] of B-doped (100) Si substrates with a typical resistivity of 2–5 Ω cm (p^- type Si), resulting in PSi layers with ~67–73% porosity and 7 nm mean pore diameter. Si substrates with a resistivity of 20–30 mΩ cm (p^+ type Si) were used to etch freestanding PSi layers having 15 nm mean pore diameter and ~64% porosity. The porosity was measured gravimetricly. The pore size distribution was derived via standard BJH method.[8] To form metal NPs, PSi was immersed in alcoholic metal salt solutions as they can uniformly wet the H-terminated hydrophobic PSi surface. The metal salt is reduced by hydrogen on the PSi surface which results in metal NP formation and HCl synthesis during the reaction.[9,10] Optical transmission spectra of PSi were measured to detect the spectral position of the peak of the dipolar LSPR. Extinction spectra were obtained by normalizing the transmission spectra of sample layers after formation of metal NPs to those of the initial ones.

We first used PSi layers prepared from p^- type Si as host for the growth of Au NPs. A low concentration (0.1 mM) of the Au precursor ($HAuCl_4$) in ethanol is used so that Au NPs grow slowly. Their growth can be monitored *in situ* by measuring the extinction spectra [see Fig. 1(a)].

In order to estimate the size of Au NPs formed, transmission electron microscope (TEM) images of the Au/PSi samples were acquired. Figure 1(b) shows an example of Au NPs formed in a PSi matrix after 40 min of exposure to the 0.1 mM $HAuCl_4$ solution in ethanol. It shows that Au NPs formed in PSi matrix have diameters <10 nm, which correlates well with the ~7 nm mean pore size. Additional atomic resolution studies demonstrate that the size of major fraction of formed metal nanoparticles is indeed below 10 nm.

As the Au NPs in Fig. 1(b) are spherical, we used Mie theory[11] to gain more detailed information about the NPs embedded in the matrix. Mie theory is an analytical solution to Maxwell's equations used to describe the interaction of

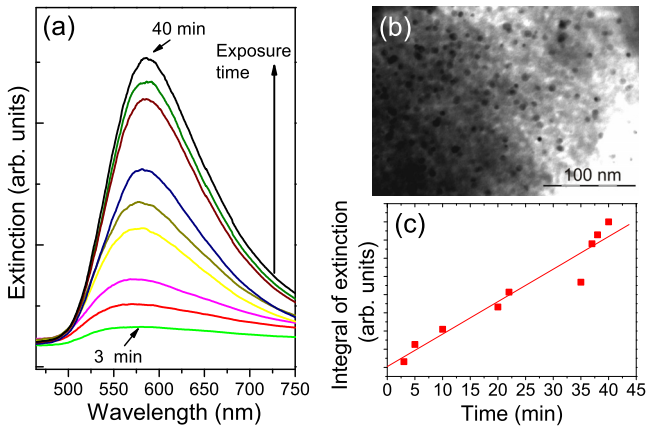

FIG. 1. (Color online) PSi layers exposed to 0.1 mM $HAuCl_4$ solution. (a) Extinction spectra of Au NPs vs exposure time. (b) TEM image of a Au/PSi sample after 40 min of exposure. (c) Integrated area under extinction spectra vs exposure time.

a)Electronic mail: s.polisski@bath.ac.uk.

light with spheres of arbitrary radius and composition, which can be used to model the LSPR of metal NPs. PSi can be described as an effective medium, where the spatial variation in the refractive index of the material is much smaller than the wavelength of light. For PSi this is generally true, but may no longer be the case once PSi is doped with metal NPs due to the confined nature of the electromagnetic field around a metal NP. Therefore, the local refractive index needs to be considered.

The Bruggemann approximation[11] is used to calculate a local effective refractive index n ~1.9–2.1 for PSi, being in a good agreement with nonlocal measured values. Using Mie theory and n, the LSPR of small Au NPs is calculated to be at ~570–590 nm [compare with experimental data in Fig. 1(a)].

The area under the extinction spectrum shows a linear increase with time during the reaction [line in Fig. 1(c)]. Using Mie theory a linear increase in the area underneath extinction spectra can be due to an increase in the number of particles in an ensemble or due to an increase in particle size. We mainly attribute the experimentally observed linear increase in to the formation of a large number of small particles rather than to the continuous growth of a constant number of NPs.

If high concentrations of salt solution are used (10 mM) we observe after ~3 min that the extinction spectra do not change significantly with time (saturation behavior). This phenomenon can be attributed to the fact that after the consumption of surface-bonded hydrogen no more Au salt can be reduced in PSi. The time frame for low resolution measurements was intentionally selected, as in this case the difference in saturation between low and high salt concentration regimes is clearly seen. The saturation, in case of low concentrated solutions, will occur after several hours, allowing controlling the growth of metal NPs.

In order to understand the effect of solution concentration and pore size distribution on the formation of Au NPs we exposed freestanding PSi layers, made from p^+ type Si substrates, for 20 min to different concentrations of $HAuCl_4$ solutions (0.1–1 mM) to achieve various loading levels of Au in PSi. After Au deposition, half of the PSi samples were oxidized in air at 1100 °C for 1 h, to form a $PSiO_2$ host, which is transparent in the spectral range of interest. The maxima of the LSPR spectra in oxidized PSi layers are blue-shifted compared to those incorporated in PSi due to a change in the local refractive index of the host (reduction of n to ~1.4). Since the LSPR of Au NPs can be clearly seen in the oxidized samples, they remain stable during a high temperature treatment.

Bimetallic Au–Pt NPs have recently been demonstrated for use in a number of applications including SERS (Ref. 12) and catalysis.[13] In this paper we show that bimetallic NPs can also be synthesized by the reduction in mixtures of metal salts in PSi. PSi, prepared from p^+ type Si substrates, was exposed for 20 min to a mix of $HAuCl_4$ and $PtCl_4$ in ethanol (different relative concentrations, in total 1 mM). The PSi layers were impregnated with three different molar ratios of Au: Pt (1:1, 1: 2, and 1: 3) before being annealed to obtain $PSiO_2$. The extinction spectra plotted in Fig. 2(a) represent samples with 3 wt % metal loading with respect to Si mass and appear as a broad, but single peak, which shifts to shorter wavelength with increased Pt concentration.

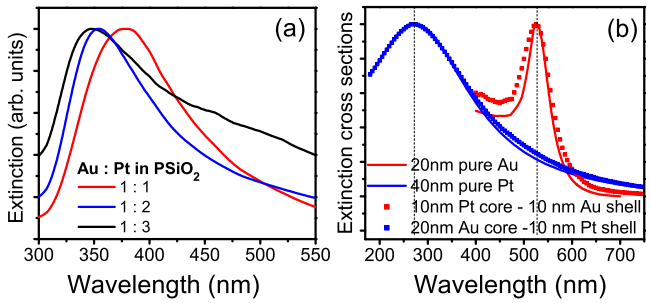

FIG. 2. (Color online) (a) Extinction spectra for metal NPs in $PSiO_2$ (formed in PSi, exposed to a Au/Pt salt mixture, and then annealed). (b) Calculated normalized extinction cross sections for Pt and Au NPs as well as core shell particles.

We have to consider three possibilities when two metal salts are simultaneously reduced in the PSi matrix: formation of (i) pure metal NPs, (ii) core-shell NPs, or (iii) alloy NPs. To interpret the experimental results in Fig. 2(a), we use Mie theory and a local refractive index n ~1.4 for $PSiO_2$. Using published data for Au (Ref. 14) and Pt,[15] pure Pt and pure Au NPs, whose size is of the order of the pore size (~15 nm), have a resonance at ~280 nm and ~525 nm, respectively [see Fig. 2(b)]. For a pure Pt NP to have a resonance at ~350 nm, its diameter should be ~70 nm, which is much larger than the mean pore size of PSi and the NP size observed by TEM. Having confirmed that the resonance at ~350 nm cannot be due to pure metal NPs, we consider the optical properties of core/shell NPs, whose LSPR peak position is governed by the shell [see Fig. 2(b)]. We focus on Au core/Pt shell NPs, as a Au coated Pt NP cannot have a resonance at ~350 nm. As with pure metal NPs, a Au NP with a Pt shell would have to be much larger than the mean pore size of PSi to have a peak at ~350 nm. Having exhausted (i) and (ii), we have to consider the formation of Au–Pt alloy NPs.

Although the optical constants of pure metals have been published,[14,15] there is no data in the literature for the optical properties of Au–Pt alloys. However, the optical properties of Au–Ag alloys have been widely studied.[6,16,17] We therefore begin by outlining the results for Au–Ag NPs using Mie theory and a linear effective dielectric function for the metal:

$$\epsilon(x) = (1 - x)\epsilon_y + x\epsilon_{Au}, \quad (1)$$

where x is the percentage of Au and y is either Ag or Pt.[16,17] We use published data for Au,[14] Ag,[14] and Pt.[15]

Using Mie theory and varying $\epsilon(x)$ for Au–Ag from 100% Ag (black) to 100% Au (cyan) in Fig. 3(a) in steps of 20% the optical properties of Au–Ag bimetallic NPs vary linearly. The linear change in the calculated LSPR peak position of Au–Ag bimetallic NPs is in agreement with experiments.[6,16,17] Applying the same approach to Au–Pt NPs, the calculated LSPR peak positions, shown in Fig. 3(b), do not shift linearly from 100% Pt (black) to 100% Au (cyan) when an effective dielectric function is used for the metal. In order to understand why the calculated LSPR peak positions of Pt–Au bimetallic particles do not vary linearly, we calculated the optical properties of other bimetallic combination of noble metals, such as Ag–Pt, Pt–Pd, Pt–Cu, and Au–Cu using published data for pure metals[14,15] and Eq. (1). We found that the calculated optical properties of bimetallic NPs only vary linearly when the real part of the dielectric

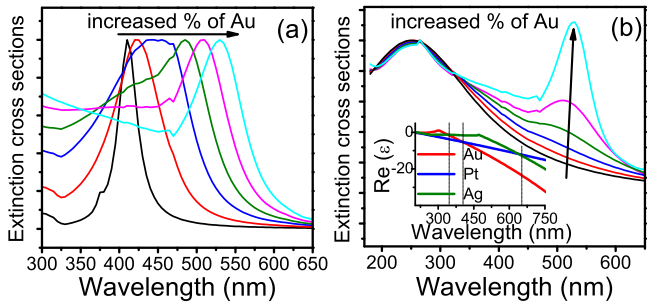

FIG. 3. (Color online) Calculated normalized extinction cross sections for (a) Ag–Au NPs and (b) Pt–Au NPs, where the dielectric function of the metal was modeled as an effective medium. Black curves are: (a) 100% Ag and (b) 100% Pt with Au concentration increasing in 20% steps to 100% Au (cyan). Inset: real part of the dielectric function for Au, Pt, and Ag (Refs. 14).

functions of the two metals do not cross. Considering the inset in Fig. 3(b) the real part of the dielectric functions of Pt and Au cross in the wavelength region close to the LSPR of Au–Pt alloy, leading to nonlinear behavior in the calculated optical properties plotted in Fig. 3(b). In the inset in Fig. 3(b) the real part of the dielectric functions of Au and Ag are parallel at long wavelengths but overlap at ~370 nm. A linear change in the calculated LSPR above 370 nm is calculated, but nonlinear behavior at and below this wavelength is observed [Fig. 3(a)]. Therefore, although the optical properties of bimetallic Au–Ag NPs calculated using an effective index for the metal appears to match experiment,[6,16,17] this only occurs as the real part of the dielectric for Au and Ag do not cross in the wavelength region close to the LSPR. We therefore conclude that effective dielectrics should not be used to model the optical properties of bimetallic alloy NPs, as previously suggested.[16] It was not possible to model the LSPR measured at ~350 nm in Fig. 2(a) using an effective dielectric function for Au–Pt. Since this peak cannot be related to (i) or (ii), we conclude that this LSPR is due to the formation of Au/Pt alloy NPs.

We have presented a method of growing Au and Au–Pt bimetallic NPs by using the chemical reductive potential of extended hydrogen-terminated surface of PSi layers. We showed that PSi matrix defines the size of formed metal NPs. Their size can also be controlled by varying the exposure time to the salt solutions and the solution concentration. We demonstrated that optical measurements enable the monitoring of noble metal NPs formation *in situ*. It was demonstrated that the formation mechanism of bimetallic NPs is the same as for the monometallic NPs and that their composition can be controlled by appropriate choice of metal salt concentration and their ratios.

This work was supported by the Engineering and Physical Sciences Research Council (EPSRC) Grant No. EP/F018622/1.

[1]S. Maier, *Plasmonics: Fundamentals and Applications* (Springer Science + Business Media LLC, New York, 2007).
[2]J. Kneipp, H. Kneipp, and K. Kneipp, Chem. Soc. Rev. **37**, 1052 (2008).
[3]H. A. Atwater and A. Polman, Nature Mater. **9**, 205 (2010).
[4]E. M. Larsson, C. Langhammer, I. Zoric, and B. Kasemo, Science **326**, 1091 (2009).
[5]*Nanoparticles and Catalysis*, edited by D. Astruc (Wiley, New York, 2007).
[6]J. F. Hund, M. F. Bertino, G. Zhang, C. Sotirion-Leventis, and N. Leventis, J. Non-Cryst. Solids **350**, 9 (2004).
[7]A. G. Cullis, L. T. Canham, and P. D. J. Calcott, J. Appl. Phys. **82**, 909 (1997).
[8]E. P. Barrett, L. G. Joyner, and P. P. Halenda, J. Am. Chem. Soc. **73**, 373 (1951).
[9]S. Polisski, B. Goller, A. Lapkin, S. Fairclough, and D. Kovalev, Phys. Status Solidi (RRL) **2**, 132 (2008).
[10]I. Coulthard and T. K. Sham, Solid State Commun. **105**, 751 (1998).
[11]C. F. Bohren and D. R. Huffman, *Absorption and Scattering of Light by Small Particles* (Wiley, New York, 1983).
[12]T. Takenaka and K. Eda, J. Colloid Interface Sci. **105**, 342 (1985).
[13]C. Mihut, C. Descorme, D. Duprez, and M. D. Amirdis, J. Catal. **212**, 125 (2002).
[14]P. B. Johnson and R. W. Christy, Phys. Rev. B **6**, 4370 (1972).
[15]*Handbook of Optical Constants of Solids*, edited by E. D. Palik (Academic Press, London, 1985).
[16]S. Link, Z. L. Wang, and E. L. Al-Sayed, J. Phys. Chem. B **103**, 3529 (1999).
[17]J. Sanchez-Ramirez, U. Pal, L. Nolasco-Hernandez, J. Mendoza-Alvares, and J. A. Pescador-Rojas, J. Nanomater. **2008**, 1.